Interference with Sin3 function induces epigenetic reprogramming and differentiation in breast cancer cells

Eduardo F. Farias[a,1], Kevin Petrie[b,1], Boris Leibovitch[a], Janice Murtagh[a], Manuel Boix Chornet[b], Tino Schenk[b], Arthur Zelent[b], and Samuel Waxman[a,2]

[a]Department of Medicine, Division of Hematology and Oncology, Tisch Cancer Center, Mount Sinai School of Medicine, New York, NY 10029; and [b]Section of Haemato-Oncology, Institute of Cancer Research, Sutton, Surrey SM2 5NG, United Kingdom

Communicated by Zhu Chen, Shanghai Institute of Hematology, Shanghai, China, May 15, 2010 (received for review November 9, 2009)

Sin3A/B is a master transcriptional scaffold and corepressor that plays an essential role in the regulation of gene transcription and maintenance of chromatin structure, and its inappropriate recruitment has been associated with aberrant gene silencing in cancer. Sin3A/B are highly related, large, multidomian proteins that interact with a wide variety of transcription factors and corepressor components, and we examined whether disruption of the function of a specific domain could lead to epigenetic reprogramming and derepression of specific subsets of genes. To this end, we selected the Sin3A/B-paired amphipathic α-helices (PAH2) domain based on its established role in mediating the effects of a relatively small number of transcription factors containing a PAH2-binding motif known as the Sin3 interaction domain (SID). Here, we show that in both human and mouse breast cancer cells, the targeted disruption of Sin3 function by introduction of a SID decoy that interferes with PAH2 binding to SID-containing partner proteins reverted the silencing of genes involved in cell growth and differentiation. In particular, the SID decoy led to epigenetic reprogramming and reexpression of the important breast cancer-associated silenced genes encoding E-cadherin, estrogen receptor α, and retinoic acid receptor β and impaired tumor growth in vivo. Interestingly, the SID decoy was effective in the triple-negative M.D. Anderson-Metastatic Breast-231 (MDA-MB-231) breast cancer cell line, restoring sensitivity to 17β-estradiol, tamoxifen, and retinoids. Therefore, the development of small molecules that can block interactions between PAH2 and SID-containing proteins offers a targeted epigenetic approach for treating this type of breast cancer that may also have wider therapeutic implications.

E-cadherin | estrogen receptor | triple-negative | Sin3 interaction domain

In recent years, the importance of the role of epigenetic abnormalities in breast cancer and cancer in general, often resulting in inappropriate gene silencing, has come to be appreciated (1). There are many examples of deregulated expression of individual genes arising from aberrant epigenetics involving changes in DNA methylation (2) and modification of the core histone proteins (3). Deregulated histone deacetylase (HDAC) activities represent one important component of the mechanism(s) underlying gene silencing in cancer. HDACs, however, do not interact directly with chromatin and are instead recruited through multi-subunit corepressor complexes that bind to transcription factors or other elements of the cellular epigenetic machinery. The HDAC1/2-containing corepressor complex is the main route by which deacetylation of chromatin-associated histones takes place, and the key adaptor protein in this complex is Sin3 (4). In mammals, there are two highly homologous Sin3 isoforms, Sin3A and B, which were originally identified as MAD binding proteins (5, 6). Sin3A/B are large multidomain proteins that contain four paired amphipathic α-helices (PAH) known as PAH domains, a central HDAC interaction domain (HID) to which almost all of the core corepressor components bind, and a C-terminal highly conserved region (HCR). As well as serving as a bridge between transcription factors and HDAC activity, the Sin3 complex has also been shown to interact with the methylated DNA binding protein MeCP2 and the HDAC3-associated corepressor silencing mediator of retinoic acid and thyroid hormone receptor (SMRT) (4). These findings implicate Sin3 proteins in a wider range of chromatin/epigenetic activities than merely histone deacetylation.

Although drugs that inhibit the enzymatic activity of HDACs (HDACi) initially held great promise, a persistent problem has been an inability to develop inhibitors with specificity for individual HDAC isotypes (with the exception of HDAC6) (7). This is also true of drugs that target the activity of DNA methyltransferases (DNMTi) and may have played a part in the limited success achieved thus far with HDACi and DNMTi in clinical applications (7). Until better epi-drugs targeting such enzymatic activities are developed, alternative strategies that target abnormal epigenetic states associated with chromatin modifiers recruited by a given oncoprotein must be pursued. One potential avenue of investigation is to use drugs to target the oncoprotein for degradation. That this rationale can be successful is exemplified by the finding that the dramatic therapeutic breakthrough in the treatment of promyelocytic leukemia protein (PML)/retinoic acid receptor α (RARα)-associated acute promyelocytic leukemia is underpinned by the targeted degradation of the fusion oncoprotein by all-*trans* retinoic acid (ATRA) and arsenic trioxide (8). Small molecule drugs that block specific protein–protein interactions offer another possibility by, for example, targeting the ability of a given oncoprotein to recruit corepressor complexes to DNA as has been recently shown for B cell leukemia 6 (BCL6) (9). We reasoned that Sin3A/B also represented a target for this approach, and to this end, we selected the well-characterized PAH2 domain, which binds with high affinity to a small number of mSin3A interaction domain (SID)-containing transcription factors in addition to MAD (4), for investigation in breast cancer models.

Here, we report that the introduction of a SID decoy interfered with binding of Sin3 PAH2 domain to partner proteins, inducing profound phenotypic changes in human and mouse breast cancer cells both in vitro and in vivo. Underlying these changes was the epigenetic reprogramming and reexpression of silenced genes encoding proteins associated with cell growth and differentiation, such as E-cadherin, estrogen receptor α (ERα), and RARβ, and with restoration of estradiol and retinoids responsiveness in triple-negative (i.e., negative for expression of estrogen and progesterone receptors and human epidermal growth factor receptor 2 [HER2]) MDA-MB-231 cell line.

Author contributions: E.F.F., K.P., B.L., J.M., A.Z., and S.W. designed research; E.F.F., K.P., B.L., J.M., M.B.C., and T.S. performed research; E.F.F., K.P., B.L., J.M., A.Z., and S.W. analyzed data; and E.F.F., K.P., B.L., A.Z., and S.W. wrote the paper.

The authors declare no conflict of interest.

[1]E.F.F. and K.P. contributed equally to this work.

[2]To whom correspondence should be addressed. E-mail: Samuel.Waxman@mssm.edu.

This article contains supporting information online at www.pnas.org/lookup/suppl/doi:10.1073/pnas.1006737107/-/DCSupplemental.

CELL BIOLOGY

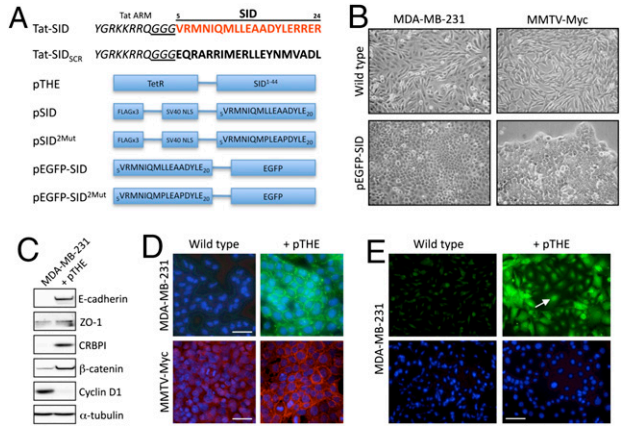

Fig. 1. Expression of a decoy peptide corresponding to MAD SID induces markers of differentiation and contact inhibition in MDA-MB-231 breast cancer cells. (*A*) Schematic of the SID peptides and expression constructs used in this study. Shown in *Upper* are the design and sequence of the Tat-SID peptide and Tat-SID$_{SCR}$ scrambled control. The Tat-SID peptide corresponds to amino acids 5–24 of MAD (indicated in red). This sequence binds Sin3 PAH2 with high affinity (32) and has been previously used to study SID-PAH2 interactions in vitro (33). Peptides contain a leader sequence (YGRKKRRQGGG) corresponding to the HIV type 1 Tat arginine-rich RNA-binding motif (ARM), which has been mutated (RRR > GGG) to improve nuclear entry (34). (*B*) Morphological changes induced by SID in MDA-MB-231 and MMTV-Myc. The expression of the SID construct induced a cobblestone-like monolayer with well-defined cell–cell contact in contrast to the vector-control transfected cells with a spindle-shape typical of fully transformed epithelial cells. pSID expresses the minimal MAD SID (amino acids 5–20) with N-terminal SV40 nuclear localization signal (NLS) and a triple FLAG epitope. (Scale bar, 100 μm.) (*C*) Western analysis of expression of the indicated proteins and gene expression in MDA-MB-231 control or expressing SID. (*D*) Confocal IF analyses showing the reexpression of membrane-associated E-cadherin induced by the expression of SID in MDA-MB-231 cells (green) and MMTV-Myc cells (red). (*E*) Reexpression of nuclear RARβ in MDA-MB-231 cells detected by immunofluorescence microscopy. (Scale bar, 25 μm.) DAPI staining (blue).

Results

SID Overexpression Induces Growth Inhibition and Differentiation of Breast Cancer Cells. To interfere with interactions between the transcriptional corepressor Sin3 and partner proteins that are mediated via the Sin3 PAH2 domain, we constructed two mammalian expression vectors containing the SID motif (Fig. 1*A*) and used the previously described pTHE vector (10), which expresses SID as a fusion with the tetracycline repressor (TetR). We also designed cell-penetrating peptides encoding the SID amino acid sequence and a scrambled control sequence to target the PAH2 domain (Fig. 1*A*). Dramatic phenotypic changes were observed in human MDA-MB-231 and mouse mammary tumor virus (MMTV)-Myc mouse breast cancer cells carried in culture after stable transfection with the three vectors expressing SID or treated with the SID peptide switching from a spindle-shaped morphology with no defined cell–cell contacts to cobblestone monolayers and well-defined cell–cell contact accompanied by cell-growth contact inhibition (Fig. 1*B*). Biochemical analysis showed an increase in the expression of E-cadherin, membrane-associated β-catenin, and zona occludens-1 (ZO-1), all of which are involved in cell-contact inhibition (Fig. 1 *C* and *D*) (11). Other differentiation-related proteins were induced such as nuclear-localized RARβ (Fig. 1*E*) and cellular retinol binding protein-1 (CRBP1) (Fig. 1*C*), both RARα target genes. Consistent with growth arrest was a marked reduction of cyclin D1 (Fig. 1*C*) (12–14). No changes in cell morphology, growth, or survival were observed in the E-cadherin–positive MCF-10A immortalized normal breast cell line transfected with any of the construct-expressing SID or treated with the SID peptide, suggesting that these changes in the phenotype are specific to transformed cells (Fig. S1).

SID and SID Peptide Block the Interaction Between MAD SID Domain and PAH-2 Domain of Sin3 and Inhibit Sin3 Activity. To confirm that the presence of the MAD SID decoy peptide or expression of the SID sequence (Fig. 1*A*) blocked the interactions between Sin3 PAH2 and partner proteins, we tested its activity in both in vitro and in vivo models (Fig. 2). As predicted, the introduction of

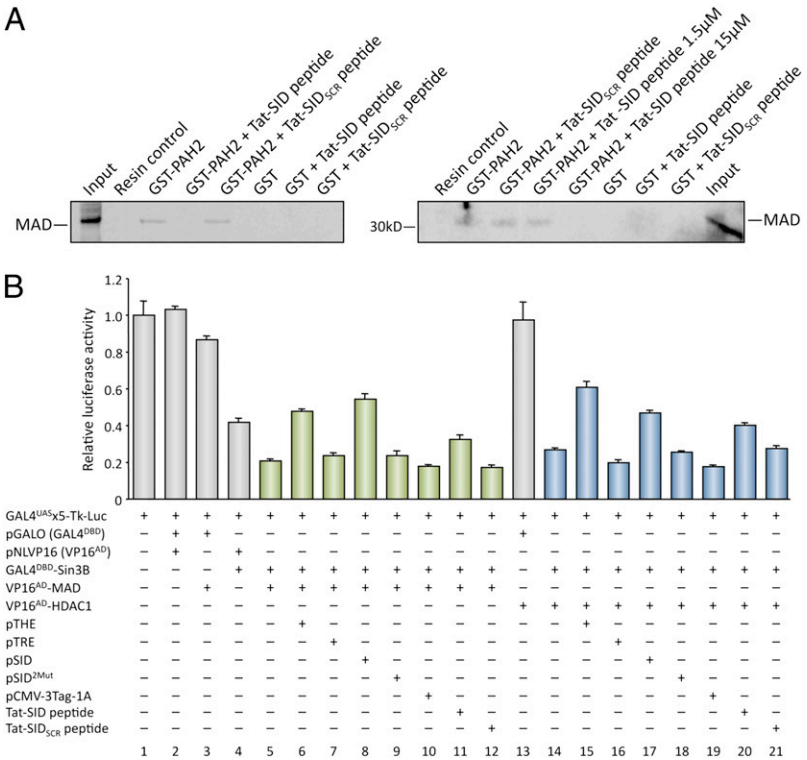

Fig. 2. SID decoy peptide blocks interactions between Sin3 PAH2 and MAD and interferes with recruitment of members of the Sin3 corepressor complex. (*A*) GST pull-down of MAD by the Sin3A PAH2 domain is blocked by SID peptide. Sin3A PAH2 domain (amino acids 306–450) was expressed in *Escherichia coli* as a GST fusion and used in a pull-down assay for in vitro interaction with [^{35}S]methionine-labeled MAD (*Left*) or MAD immunoprecipitated from MDA-MB-231 cell lysates (*Right*); 25% of input is shown for in vitro-translated MAD and 10% of input for immunoprecipitated MAD (input). Assays were performed using 15 μM Tat-SID or Tat-SID$_{SCR}$ peptide unless otherwise indicated. (*B*) Mammalian two-hybrid analysis shows that SID interferes with recruitment of MAD and HDAC1 by Sin3B; 293T cells were transfected with GAL4^{uas}x5-Tk-Luc reporter together with mammalian two-hybrid vectors expressing a fusion of Sin3B with GAL4 DNA binding domain (GAL4^{DBD}) and fusions of MAD and HDAC1 (columns highlighted in green and blue, respectively) with VP16 activation domain (VP16^{AD}), as well as SID expression vectors, as indicated. Samples transfected with a vector expressing mutated SID (pSID^{2Mut}) and pTRE and pCMV-3Tag-1A empty vectors were included as negative controls. Luciferase activity was normalized by cotransfection of Renilla luciferase. The parent GAL4DBD and VP16AD mammalian two-hybrid vectors (pGALO and pNLVP16, repectively) (35), were also used as negative controls. The basal value was set to 1. Values of relative luciferase activity and error bars represent the averages and SDs, respectively, of four separate experiments. Transfection of the pM3-VP16(AD) positive control vector (Clontech), a fusion of GAL4^{DBD} and VP16^{AD}, resulted in a large (60-fold) increase in relative luciferase activity (not shown). Where indicated, samples were treated with 15 μM Tat-SID or Tat-SID$_{SCR}$ peptide at time of cell plating and after transfection.

SID peptide but not a scrambled control blocked interactions between the PAH2 domain of Sin3A and both in vitro-translated MAD (Fig. 2) and MAD immunoprecipitated from SID peptide-treated MDA-MB-231 cells (Fig. 2 *Right*). This result was confirmed in 293T cells using the mammalian two-hybrid system (Fig. 2*B*). Coexpression of GAL4^{DBD}-Sin3B and VP16^{AD}-MAD caused a 5-fold decrease in luciferase activity on a reporter under the control of GAL4^{UAS} elements (Fig. 2*B*, column 5). This repression, despite the presence of the VP16 activation domain fused to MAD, is consistent with previously reported data (15). Consistent with the in vitro data, expression of the MAD SID peptide sequence from vectors encoding FLAG (DYKDDDDK epitope)-tagged SID and a fusion of TetR and SID led to a 2-fold increase in luciferase activity compared with that found with GAL4^{DBD}-Sin3B and VP16^{AD}-MAD coexpression (Fig. 2*B*, columns 6 and 8). This result was also confirmed, albeit to a lesser degree, by applying SID peptide to the cell-culture medium (Fig. 2*B*, column 11). Neither coexpression of doubly mutated SID nor addition of scrambled control peptide led to an increase in luciferase activity. To determine whether the SID decoy peptide interfered exclusively with interactions between Sin3 PAH2 and its partner proteins or had a wider effect on assembly of the Sin3 corepressor complex, we also tested the effect of the SID decoy on luciferase activity resulting from coexpression of GAL4^{DBD}-Sin3B and VP16^{AD}-HDAC1 (Fig. 2*B*, columns 14–21). Interestingly, the data obtained were very similar to those for GAL4^{DBD}-Sin3B and VP16^{AD}-MAD. This was found for the TetR–SID fusion (28.4 kDa) (Fig. 2*B*, column 15) but also, to a somewhat lesser degree, the smaller FLAG-tagged SID (6.6 kDa) (Fig. 2*B*, column 17) as well as the SID peptide (Fig. 2*B*, column 20). Thus, the SID decoy peptide can effect not only binding of Sin3-PAH2 partner proteins but also recruitment of HDAC1 and potentially, additional factors that do not interact with Sin3 through the PAH2 domain.

Induction of Morphogenesis by the SID Peptide in Triple-Negative Breast Cancer Cells. To determine the extent of the reversion of the transformed phenotype in MDA-MB-231 and MMTV-Myc cells, 3D cultures in basement membrane matrix (Matrigel; BD Biosciences) were prepared to examine the morphogenetic potential of the SID peptide expression in these cell lines. Stable transfected cells expressing the empty vector, the SID amino acid sequence, or a double mutant incapable of binding the PAH2 domain of Sin3 (SID-L12P/A16P) were seeded in quadruplicates (5×10^3 cells/well) on Matrigel following the protocol described by Debnath et al. (16). Phase contrast and confocal immunofluorescence (IF) analysis indicated that the highly invasive phenotype exhibited by both cell lines (star-like colonies) was blocked only in SID-expressing cells (smooth, round colonies). The quantification of this (5 fields/well) indicates that about only 15% of the colonies retained a mild invasive phenotype (Fig. 3*A*). The confocal analysis revealed that about 25% of the MDA-MB-231 SID-expressing colonies underwent acinar morphogenesis but with poor polarization (Fig. 3*A Middle*). Although the MMTV-Myc cells displayed a strong reduction in the invasive phenotype, few colonies showed rudimentary lumen formation with abnormal polarization (Fig. 3*A Right*). Similar results were obtained by treating the MDA-MB-231 cells with the cell-penetrating SID peptides; interestingly, besides decreasing the number of the colonies with invasive phenotype by ~80%, the number and size of the colonies were reduced when cultures were exposed to 5 μM SID (Fig. 3*B Lower*). As expected, the negative control scrambled (SID$_{SCR}$) peptide did not exert this effect (Fig. 3*B* Lower). These sets of results indicate that it is possible to induce a substantial degree of differentiation and morphogenesis in triple-negative cell lines by selective interference with the Sin3 activity.

SID Induces Antitumor Effect in Vivo. To study the in vivo antiproliferative effect of SID decoy, MMTV-Myc cells with stable

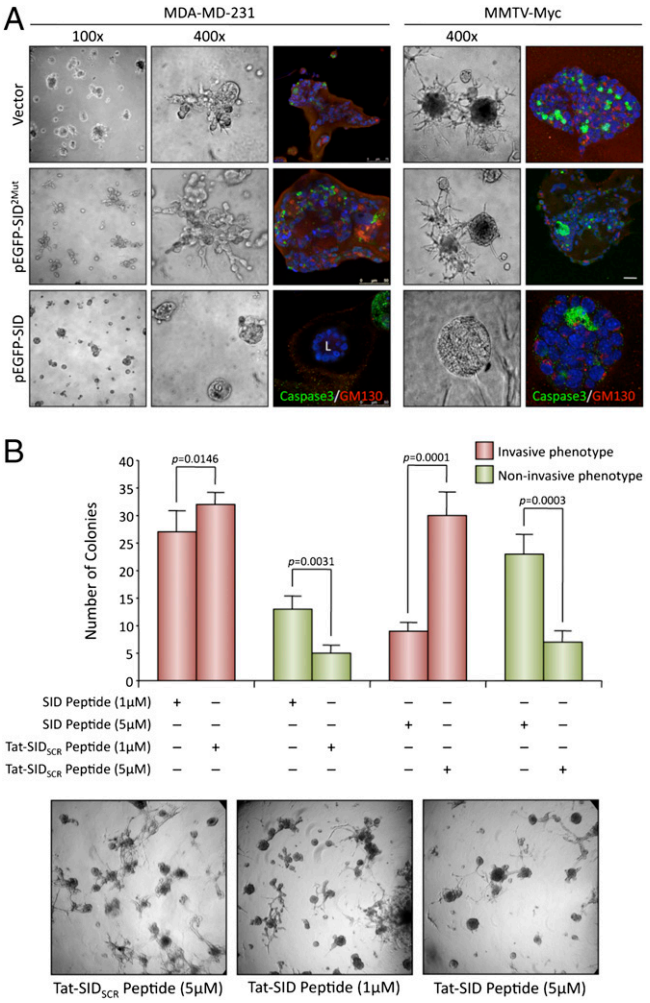

Fig. 3. (*A*) Morphogenesis in 3D cultures in Matrigel. MDA-MB-231 and MMTV-Myc cells expressing SID or the double mutant were cultured in 3D-Matrigel for 14 d. Both vector and the double mutant transfected cells develop large and invasive colonies (*Top* and *Middle*); meanwhile, the cells expressing SID were smaller and noninvasive. Moreover, ~25% of the MDA-MB-231 colonies displayed nonpolarized rudimental lumens (*Bottom Right*) (L, lumen). However, at 14 d in Matrigel culture, expression patterns of GM130 (red) and caspase-3 (green), polarization and cavitation markers, respectively, did not indicate full polarization of SID-expressing cells. (*B*) Reversion of the invasive phenotype of the MDA-MB-231 cells in Matrigel 3D cultures. *Upper* indicates change in numbers of invasive versus noninvasive colonies (as indicated in red- and green-colored bars, respectively) in the presence of different concentrations (as indicated) of cell penetrating SID or SID$_{SCR}$ (scrambled control) peptide. The colonies were counted after 10 d of treatment with a medium containing fresh peptide changed every 24 h. *Lower* shows phase-contrast microscopy indicating the effect of each treatment on colony morphology. The reduction in invasive phenotype was quantified by counting five low magnification fields per well done in triplicates (*Upper*). (Scale bar, 200 μm.) The *P* value was calculated using unpaired Student *t* test.

SID expression were generated from MMTV-c-Myc tumors. MMTV-Myc cells stably expressing pTHE plasmid or SID expressed as a fusion with enhanced green fluorescent protein (pEGFP-SID) were injected into the fat pads of friend virus B-type (FVB) syngeneic mice. There was a 75% decrease in relative tumor volume 14 d later compared with the vector control (Fig. 4*A*) ($P < 0.0001$). Immunohistochemical analysis of tumors revealed that the introduction of SID decoy-induced reexpression of membrane-associated E-cadherin increased expression of the cyclin-dependent kinase inhibitor p27^{Kip1} (a marker of growth arrest) and down-regulated retinoblastoma protein (Rb) in all

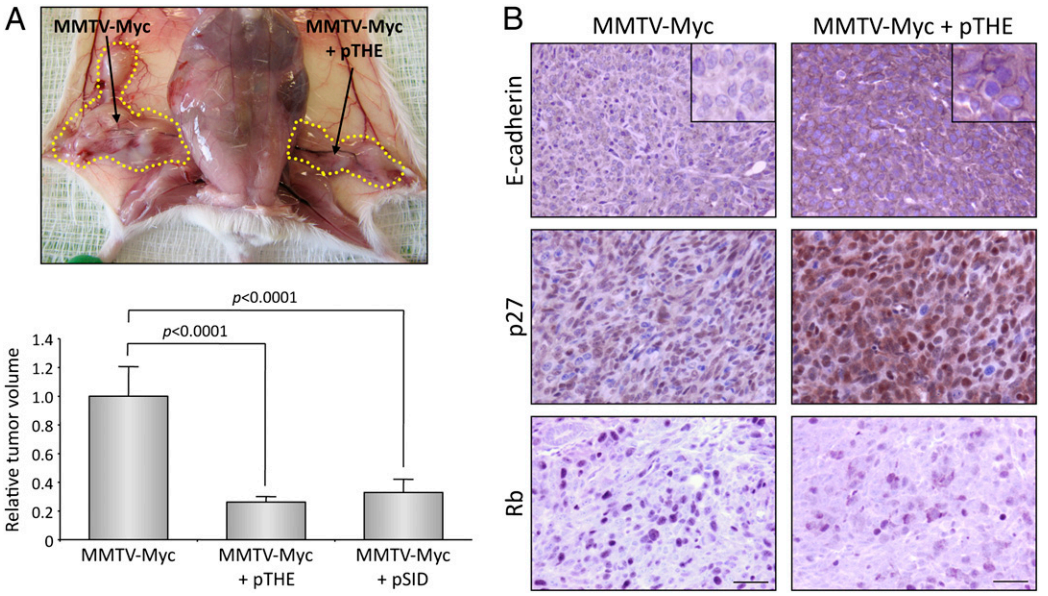

Fig. 4. Expression of the SID domain or the SID-MAD–interacting peptide fused with GFP impairs tumor growth. (*A*) MMTV-Myc cells (2.5×10^5 cells/fat pad) were injected into the mammary fat pads of FVB syngeneic mice (n = 10). MMTV-Myc cells stably expressing pTHE were injected in the left flank, with vector control injected in the right flank of each mouse as indicated to avoid interanimal variation between groups, and tumors were retrieved after 14 d. (*B*) Immunohistochemical analysis of the tumors indicates that those expressing the SID domain express higher levels of E-cadherin localized to the plasma membrane (*Top Left Inset*), higher nuclear expression of p27, and low Rb (8 of 8 tumors studied). (Scale bar, 50 μm.) Similar results were obtained using pEGFP-N3/SID plasmids.

animals examined (n = 8) (Fig. 4*B*). Caspase-3 staining revealed no differences in apoptosis, suggesting that the antitumor effect of the SID interference is mainly associated with diminished invasiveness and induction of terminal differentiation rather than through apoptosis.

SID Domain Expression Induces Early and Intense Chromatin Remodeling. Given that expression of the SID decoy peptide is associated with reexpression of genes silenced in MDA-MB-231 cells, we sought to identify epigenetic changes associated with the promoter regions of two genes that are important in the pathology of breast cancer, *CDH1* and *ESR1*, which encode E-cadherin and ERα, respectively. We found that although there was a modest increase in the overall acetylation levels of histone H3 (Fig. S2), the levels of H3K4 methylation increased dramatically, in particular for *CDH1* (Fig. 5*B*). This was accompanied by a large increase in the levels of E-cadherin and ERα expression (Fig. 5*C*). Similar results on H3K4 methylation were observed for RARβ, consistent with the reexpression shown in Fig. 1*E*. These changes were not found in the ribosomal protein L30 (RPL30) housekeeping gene used as control. Consistent with the notion that epigenetic reprogramming of silenced gene promoters occurs in response to SID decoy, compared with wild-type cells, bisulfite sequencing of the *ESR1* promoter/5′UTR revealed an average 70% loss of CpG methylation (P = 0.0095) within this region in MDA-MB-231 cells stably transfected with pSID but not $pSID^{2Mut}$ (Fig. 5*D Right* and Fig. S3 *Right*). Bisulfite sequencing analysis of the *CDH1* promoter/5′UTR showed that, compared with $pSID^{2Mut}$-transfected or wild-type MDA-MB-231 cells, there was also an average 60% decrease in the level of CpG methylation (P = 0.0031) in pSID-transfected cells. Interestingly, in the cases of both the *ESR1* and *CDH1* promoter/5′ UTRs, the most significant loss of CpG dinucleotide demethylation was focused on regions adjacent to the transcription initiation sites (Fig. 5*D Left*). It should be noted that the modest level of *CDH1* promoter methylation (~30%) in MDA-MB-231 cells found here is in line with previously reported results (17, 18).

SID Induces ER and RARβ Sensitivity to Estrogen and Retinoids. The transfection of MDA-MB-231 cells with two different SID constructs or SID peptide induced the reexpression of ERα and RARβ (Fig. 5*B*). Functionality of the ER reexpression was shown by induced growth sensitivity to 2.5 nM estradiol (E2) treatment of MDA-MB-231 cells and the prevention of E2 growth stimulation by 2.5 μM tamoxifen as measured by 3-*(4,5-Dimethylthiazol-2-Yl)*-2,5-Diphenyltetrazolium Bromide (MTT) assay (Fig. 5*E Left*). Immunofluorescence analysis also shows an increased expression of RARβ in cells transfected with SID (Fig. 1*E*). This finding coincides with the increased expression of E-cadherin and CRBP1, known RAR target genes, and the induction of p27, highly sensitive to RAR activation. Furthermore, the reexpression of RARβ is functional, because there is a significant growth inhibition of MDA-MB-231 cells by treatment with the retinoids ATRA (1 μM) and RARα-specific agonist AM580 (100 nM) (Fig. 5*E Right*). Thus, blocking specific sites of a component of a transcriptional corepressor limited to few transcription factors can be used to induce a differentiation phenotype and antitumor effect in breast cancer, and these events may impart and/or restore therapeutic targets in breast cancer.

Discussion

In this study, we provide in vitro and in vivo evidence that introduction of SID decoy peptide or expression of its corresponding sequence disrupts the interaction between the PAH-2 domain of Sin3 and MAD (and potentially, other SID-containing proteins), leading to dramatic phenotypic changes in human and mouse breast cancer cells characterized by an early increase in cell adhesion and subsequent contact inhibition. On a molecular level, in MDA-MB-231 cells, these changes are associated with induction of E-cadherin and β-catenin. Moreover, MDA-MB-231 cells expressing SID or treated with SID peptide form mainly noninvasive colonies, undergoing morphogenesis and growth inhibition. Importantly, these findings were validated in vivo using FVB syngeneic mice injected with cells derived from MMTV-c-Myc–induced tumors. In all cases, mice bearing implanted MMTV-Myc cells expressing SID decoy sequence displayed a dramatically reduced tumor burden.

Our data support the notion that these phenotypic changes are a consequence of disrupting PAH-2 Sin3–mediated functions. As yet, it is unclear whether this is specifically because of interference with Sin3 recruitment by SID-containing transcription factors or if the SID decoy can also prevent the binding of certain corepressor components to the core Sin3 complex, and further research is required to answer these questions. It is, however, clear that the reexpression of the key breast cancer-associated genes *CDH1* and *ESR1* in MDA-MB-231 cells is accompanied by extensive epigenetic reprogramming characterized by a reduction in levels of promoter hypermethylation and dramatic increases in histone H3K4 methylation, a gene-activation mark, together with increases in H3 acetylation and decreases in H3K27 trimethylation. In-

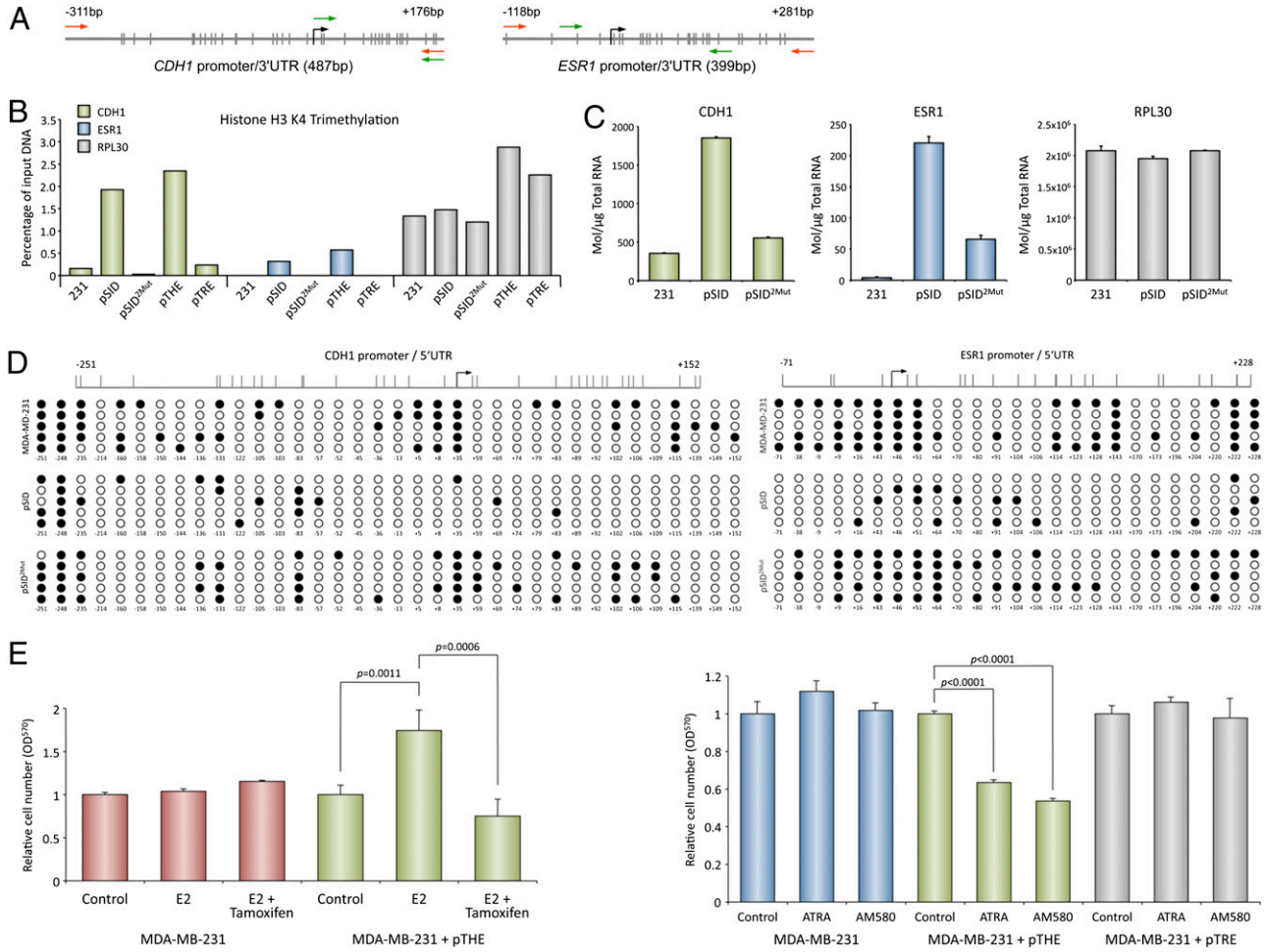

Fig. 5. (*A*) Schematic representations of the promoters and 5′UTR of *CDH1* and *ESR1* used in this study. Positions of CpG dinucleotides are indicated by gray ticks, and the transcription initiation sites are represented by black arrows. The relative positions of primer pairs used to PCR-amplify immunoprecipitated DNA from ChIP analysis (green arrows) and bisulfite-modified DNA (red arrows) are also indicated. (*B*) H3K4^{me3} levels on the CDH1 and ESR1 promoter regions increase dramatically in response to SID. ChIP analysis was performed with chromatin from wild-type or stably transfected MDA-MB-231 cells as indicated. Cross-linked protein-DNA complexes were immunoprecipitated with an antitrimethyl H3K4 antibody and amplified by real-time PCR. Results are shown as percentage of input DNA. The RPL30 housekeeping gene is shown as a control. (*C*) Real-time PCR analysis of CDH1 and ESR1 gene expression. Values are shown as molecules per microgram total RNA and were derived from the ΔCt between the GAPDH housekeeping gene and the gene of interest. The amount of GAPDH molecules per microgram total RNA was determined by absolute quantification. (*D*) The CDH1 and ESR1 promoters undergo demethylation in response to SID. After bisulfite modification of wild-type or stably transfected MDA-MB-231 cells, as indicated, specifically amplified PCR products were sequenced using primers corresponding to the promoter/5′UTR of *ESR1*. Positions of CpG dinucleotides are indicated by gray ticks, and the transcription initiation sites are indicated by black arrows. Five clones were sequenced per sample, and a black-filled circle represents where a CpG dinucleotide was found to be methylated. Unmethylated CpGs are represented by open circles. CpG positions are shown relative to transcription initiation site. (*E*) Functional assays for ERα and RAR activation. To determine whether the reexpressed ERα and RARβ were functional in MDA-MB-231 cells transfected with SID (pTHE plasmid), cell proliferation assays were performed. Cells were stimulated with 2.5 nM estradiol (E2) or E2 plus 2.5 μM tamoxifen overnight (*Left*) or 1 mM ATRA (pan-RAR agonist) or 100 nM AM580 (RARα-specific agonist) daily for 48 h (*Right*) to determine the activation of ERα and RARs, respectively.

terestingly, levels of H3K4 methylation and DNA methylation have been directly inversely linked (19, 20), with recent research showing that methylation of H3K4 prevents de novo DNA methylation DNA by blocking DNMT3L binding and recruitment of DNMT3A2 (19). Expression microarray analysis of the transcriptional program directed by introduction of the SID decoy into MDA-MB-231 cells is currently being undertaken, but given that expression of control genes is not affected, the number of genes modulated could be relatively small. This is desirable, and together with the finding that critical breast cancer genes such as *CDH1*, *ESR1*, and *RARB* are reexpressed and function in triple-negative breast cancer cells, these results could be the basis for a specific and effective treatment. Indeed, mirroring our data, the ectopic expression of E-cadherin in MDA-MB-231 cells suppresses their invasive properties (21).

Although the increase in histone H3 acetylation found with expression of the SID decoy is in line with the well-established histone deacetylase activity associated with Sin3 (4), such large increases in levels of H3K4 methylation were not anticipated. However, recent research has shown a role for Sin3 and JARID1A (Jumonji AT-rich interactive domain, also known as retinoblastoma binding protein-2 [RBP2] and K-demethylase-5A [KDM5A]), a H3K4$^{me2/me3}$ demethylase, in permanent gene silencing in myoblasts (22). It was shown that Sin3 and JARID1A directly interact and that JARID1A is associated with the *CDH1* promoter. Another JARID family member, JARID1B (PLU-1/KDM5B), which shares a high degree of homology with JARID1A, is also of great interest (23). Whereas a direct interaction with Sin3 remains to be tested, JARID1B does interact directly with histone deacetylases (24), and interestingly, it has been found to be overexpressed in breast cancers (25). Furthermore, the Drosophila homolog of JARID1A/1B, LID little imaginal discs (KDM5), interacts directly with Sin3 in gene-selective silencing (26). Both JARID1A and 1B are expressed in MDA-MB-231 cells.

However, it is perhaps most noteworthy that, in a syngeneic mouse mammary tumor model similar to the one used here, stable knockdown of JARID1B also resulted in reduced tumor cell growth (27). Thus, blocking the activity of JARID1A/B represents a strong potential candidate mechanism to explain the dramatic increases in H3K4 methylation found with SID decoy expression and warrants further investigation. Although single treatment with inhibitors of class I and II HDAC had very limited effects in MDA-231 cells (Fig. S4), it has been shown that use of inhibitors of class III HDACs (Sirtuins) leads to reexpression of E-cadherin in MDA-MB-231 cells (28). Interestingly, the reexpression of another silenced gene, *SFRP1*, in MDA-MB-231 cells was not accompanied by a loss of promoter CpG hypermethylation (28). In this study, we find the promoters of both *CDH1* and *ESR1* to not be densely methylated, and loss of DNA methylation after exposure to SID decoy is most apparent in the regions adjacent to the transcription initiation sites analyzed here for both genes. Therefore, the loss of DNA methylation may follow changes in H3K4 methylation status, and as described for Sirtuin inhibitors, reexpression of *ESR1* and *CDH1* in this case may not be strongly dependent on the removal of methylated CpGs (28). Nevertheless, it will be interesting to examine the effectiveness of SID decoy in rescuing E-cadherin and ERα expression in additional triple-negative breast cancer cell lines (or sublines of MDA-MB-231 cells where the promoters of *CDH1* and *ESR1* are more densely methylated). It also remains to be seen whether Sirtuin inhibitors (and other epi-drugs) can synergize with the SID decoy, but it is noteworthy that SIRT1 can associate with Sin3-containing corepressor complexes through an interaction with Sin-associated protein-30 (SAP30) (29).

Although current epi-drugs, such as nonspecific HDACi and DNMTi, have been shown to induce reexpression of silenced genes thought to play a role in the development of breast cancer in experimental models, with one or two exceptions, these results remain to be translated into effective therapies (30). This may be because of cytotoxicity, pleiotropic effects on a wide range of transcription factors, and an inability to induce genes required for both growth inhibition and terminal cell division. Given the substrate specificity of histone methyltransferases and demethylases relative to HDACs and DNMTs, inhibitors targeting their activities may well prove more useful in cancer therapy (31). However, the strategy with the greatest potential to target aberrant epigenetic states in a specific manner lies with using small molecules to block specific interactions between oncoproteins and epigenetic modifiers required for their oncogenic activity (9, 31). In summary, taking into consideration the data presented here and given the well-characterized nature of the interaction between SID-containing factors and Sin3 PAH2, a screen to identify small molecules that block binding may well yield drugs with therapeutic potential in breast cancer and the treatment of cancer in general.

Materials and Methods

Details of the procedures are described in *SI Materials and Methods*. The experiments were conducted with at least three replicates in at least two independent experiments. Statistical analysis was used. *P* values were calculated using the unpaired Student *t*, Mann–Whitney, or one-way ANOVA analysis as indicated.

ACKNOWLEDGMENTS. We thank Dr. T.-C. He (University of Chicago Medical Center, Chicago, IL) for pTHE and pTRE plasmids. This work was supported by the Samuel Waxman Cancer Research Foundation, the Chemotherapy Foundation, National Institutes of Health–National Cancer Institute Shared Resources Grant 5R24-CA095823-04, National Science Foundation Major Research Instrumentation Grant DBI-972404, and National Institutes of Health Shared Instrumentation Grant 1S10-RR0-9145-01 to Mount Sinai School of Medicine's Microscopy Shared Resources Facility. K.P., T.S., and A.Z were also supported by a Program Grant from Leukaemia and Lymphoma Research, UK.

1. Ting AH, McGarvey KM, Baylin SB (2006) The cancer epigenome—components and functional correlates. *Genes Dev* 20:3215–3231.
2. Frigola J, et al. (2006) Epigenetic remodeling in colorectal cancer results in coordinate gene suppression across an entire chromosome band. *Nat Genet* 38:540–549.
3. Fraga MF, et al. (2005) Loss of acetylation at Lys16 and trimethylation at Lys20 of histone H4 is a common hallmark of human cancer. *Nat Genet* 37:391–400.
4. Silverstein RA, Ekwall K (2005) Sin3: A flexible regulator of global gene expression and genome stability. *Curr Genet* 47:1–17.
5. Schreiber-Agus N, et al. (1995) An amino-terminal domain of Mxi1 mediates anti-Myc oncogenic activity and interacts with a homolog of the yeast transcriptional repressor SIN3. *Cell* 80:777–786.
6. Ayer DE, Lawrence QA, Eisenman RN (1995) Mad-Max transcriptional repression is mediated by ternary complex formation with mammalian homologs of yeast repressor Sin3. *Cell* 80:767–776.
7. Zelent A, et al. (2008) Derepression in the desert: The third workshop on clinical translation of epigenetics in cancer therapeutics. *Cancer Res* 68:4967–4970.
8. Hu J, et al. (2009) Long-term efficacy and safety of all-trans retinoic acid/arsenic trioxide-based therapy in newly diagnosed acute promyelocytic leukemia. *Proc Natl Acad Sci USA* 106:3342–3347.
9. Cerchietti LC, et al. (2009) A peptomimetic inhibitor of BCL6 with potent antilymphoma effects in vitro and in vivo. *Blood* 113:3397–3405.
10. Jiang W, et al. (2001) Tetracycline-regulated gene expression mediated by a novel chimeric repressor that recruits histone deacetylases in mammalian cells. *J Biol Chem* 276:45168–45174.
11. Cowin P, Rowlands TM, Hatsell SJ (2005) Cadherins and catenins in breast cancer. *Curr Opin Cell Biol* 17:499–508.
12. Farias EF, Marzan C, Mira-y-Lopez R (2005) Cellular retinol-binding protein-I inhibits PI3K/Akt signaling through a retinoic acid receptor-dependent mechanism that regulates p85-p110 heterodimerization. *Oncogene* 24:1598–1606.
13. Farias EF, et al. (2005) Cellular retinol-binding protein I, a regulator of breast epithelial retinoic acid receptor activity, cell differentiation, and tumorigenicity. *J Natl Cancer Inst* 97:21–29.
14. Kuppumbatti YS, Bleiweiss IJ, Mandeli JP, Waxman S, Mira-Y-Lopez R (2000) Cellular retinol-binding protein expression and breast cancer. *J Natl Cancer Inst* 92:475–480.
15. Ayer DE, Laherty CD, Lawrence QA, Armstrong AP, Eisenman RN (1996) Mad proteins contain a dominant transcription repression domain. *Mol Cell Biol* 16:5772–5781.
16. Debnath J, Muthuswamy SK, Brugge JS (2003) Morphogenesis and oncogenesis of MCF-10A mammary epithelial acini grown in three-dimensional basement membrane cultures. *Methods* 30:256–268.
17. Lombaerts M, et al. (2006) E-cadherin transcriptional downregulation by promoter methylation but not mutation is related to epithelial-to-mesenchymal transition in breast cancer cell lines. *Br J Cancer* 94:661–671.
18. Leong KG, et al. (2007) Jagged1-mediated Notch activation induces epithelial-to-mesenchymal transition through Slug-induced repression of E-cadherin. *J Exp Med* 204: 2935–2948.
19. Ooi SK, et al. (2007) DNMT3L connects unmethylated lysine 4 of histone H3 to de novo methylation of DNA. *Nature* 448:714–717.
20. Okitsu CY, Hsieh CL (2007) DNA methylation dictates histone H3K4 methylation. *Mol Cell Biol* 27:2746–2757.
21. Wong AS, Gumbiner BM (2003) Adhesion-independent mechanism for suppression of tumor cell invasion by E-cadherin. *J Cell Biol* 161:1191–1203.
22. van Oevelen C, et al. (2008) A role for mammalian Sin3 in permanent gene silencing. *Mol Cell* 32:359–370.
23. Secombe J, Eisenman RN (2007) The function and regulation of the JARID1 family of histone H3 lysine 4 demethylases: The Myc connection. *Cell Cycle* 6:1324–1328.
24. Barrett A, et al. (2007) Breast cancer associated transcriptional repressor PLU-1/JARID1B interacts directly with histone deacetylases. *Int J Cancer* 121:265–275.
25. Barrett A, et al. (2002) PLU-1 nuclear protein, which is upregulated in breast cancer, shows restricted expression in normal human adult tissues: A new cancer/testis antigen? *Int J Cancer* 101:581–588.
26. Moshkin YM, et al. (2009) Histone chaperones ASF1 and NAP1 differentially modulate removal of active histone marks by LID-RPD3 complexes during NOTCH silencing. *Mol Cell* 35:782–793.
27. Yamane K, et al. (2007) PLU-1 is an H3K4 demethylase involved in transcriptional repression and breast cancer cell proliferation. *Mol Cell* 25:801–812.
28. Pruitt K, et al. (2006) Inhibition of SIRT1 reactivates silenced cancer genes without loss of promoter DNA hypermethylation. *PLoS Genet* 2:e40.
29. Binda O, Nassif C, Branton PE (2008) SIRT1 negatively regulates HDAC1-dependent transcriptional repression by the RBP1 family of proteins. *Oncogene* 27:3384–3392.
30. Dworkin AM, Huang TH, Toland AE (2009) Epigenetic alterations in the breast: Implications for breast cancer detection, prognosis and treatment. *Semin Cancer Biol* 19:165–171.
31. Petrie K, Zelent A, Waxman S (2009) Differentiation therapy of acute myeloid leukemia: Past, present and future. *Curr Opin Hematol* 16:84–91.
32. van Ingen H, et al. (2004) Extension of the binding motif of the Sin3 interacting domain of the Mad family proteins. *Biochemistry* 43:46–54.
33. Le Guezennec X, Vriend G, Stunnenberg HG (2004) Molecular determinants of the interaction of Mad with the PAH2 domain of mSin3. *J Biol Chem* 279:25823–25829.
34. Cardarelli F, Serresi M, Bizzarri R, Beltram F (2008) Tuning the transport properties of HIV-1 Tat arginine-rich motif in living cells. *Traffic* 9:528–539.
35. Kato GJ, Barrett J, Villa-Garcia M, Dang CV (1990) An amino-terminal c-myc domain required for neoplastic transformation activates transcription. *Mol Cell Biol* 10: 5914–5920.